Applied Chemical Engineering (2023) Volume 6 Issue 2
doi: 10.24294/ace.v6i2.2366

ORIGINAL RESEARCH ARTICLE

The effects of combustion phasing induced by water injection on deNOx performance of GDI engine at MBT ignition timing

Nuttapon Buntek[1,2], Kampanart Theinnoi[1,2], Sak Sittichompoo[1,2,*]

[1] *College of Industrial Technology, King Mongkut's University of Technology North Bangkok, Bangkok 10800, Thailand*

[2] *Research Centre for Combustion Technology and Alternative Energy (CTAE), Science and Technology Research Institute, King Mongkut's University of Technology North Bangkok, Bangkok 10800, Thailand*

*** Corresponding author:** Sak Sittichompoo, sak.s@cit.kmutnb.ac.th

ABSTRACT

The call for greenhouse gas emission reduction as the result of global warming has been the main cause of the more rigorous emission legislation in the road transportation sector. In response to such requirements, car makers opt for the 'down-sizing' trend for engine displacement with the aim to increase brake thermal efficiency by increasing engine load (mean effective pressure). However, this leads to higher potential of engine knocking and elevated NOx emissions. This study investigates the effects of combustion phasing induced by water injection via the intake manifold of a naturally aspirated GDI engine at MBT ignition timing fuelled with E20. Water up to 30% of fuel mass is port-injected during high engine load and maximum NOx reduction of up to 82% could be achieved as the result of lower RoHR caused by vaporisation of water. Water injection prolonged the ignition delay and combustion duration (CA1090) without deterioration of combustion stability (%COV of IMEP). The optimisation of ignition timing based on MBT can improve CO emission compared to EGR systems. The proposed study demonstrates the possibility to achieve low nitrogen emissions without the need of precious metal-based catalysts.

Keywords: internal combustion engine; gasoline direct injection engine; water-injection; combustion phasing; NOx emissions; alternative fuel; maximum brake torque (MBT)

ARTICLE INFO

Received: 6 July 2023
Accepted: 26 July 2023
Available online: 21 August 2023

1. Introduction

Global warming is the consequence of the elevated levels of greenhouse gas (GHG) emissions which leads to the rise of average global atmospheric temperature[1]. Global warming negatively affects the environment including human's livelihoods due to natural disasters, for instance, unbalanced water cycle creating drought, hotter and longer dry weather causing wildfire, accelerating glacier melting those results in the mean sea level rises. Transportation is one of the human's activities that releases a fair share of GHG and other pollutants into the atmosphere through the use of internal combustion engines (ICE)[2]. Pollutants emitted from ICEs, especially; particulate matter (PM) poses a public health crisis[3]. This has driven the research and development of cleaner and more efficient ICEs.

Compression ignition (CI) engines or diesel engines were popular among passenger vehicles in the past decade owing to the outstanding fuel economy compared to gasoline engine counterparts. However, the concerns about PM and NOx emissions together with the diesel-gate scandal[4] has changed the direction of research and development toward gasoline engines. Despite lower thermal efficiency due to low compression ratio and operation at stoichiometry (φ = 1)[5,6]. However; gasoline engines generate significantly lower amounts of PM[7–9] as the result of highly homogeneous combustion compared to heterogeneous combustion in diesel engines which have a higher degree of local fuel-rich zone[5]. Gasoline direct injection (GDI) engine has been developed to yield better fuel efficiency and CO/THC compared to port-injection gasoline engines.

The EU emission legislation has enforced the CO_2 emission limitation per distance travelled[10,11] which aims to reduce CO_2 emissions from passenger vehicles by 25% within 2025 (to 81 g/km). This influences GDI engines to have smaller displacement and operate at higher indicated mean effective pressure (IMEP) and at lower RPM in order to attain low brake specific fuel consumption (BSFC)[12–14]. Increasing IMEP can be achieved by turbocharging which significantly increases intake air pressure and temperature. This leads to the high propensity to self-ignition or knocking[6] which creates in-cylinder pressure anomaly prior to TDC creating more negative work and results in lowered thermal efficiency. Knocking can be avoided by using rich AFR (Air-fuel ratio) to reduce intake charge temperature, and retarding ignition timing (IGT) which simultaneously reduce peak in-cylinder pressure at the expense of worsened fuel economy and engine-out pollution.

Apart from knocking problems, at high engine load, the high in-cylinder pressure and temperature can creates a large amount of thermal NOx from N_2 reacting with O_2[6]. For gasoline engines, NOx emission can be abated using a three way catalyst (TWC) at φ = 1 (net reducing condition) where high conversion of CO and THC is simultaneously obtained[15]. However, GDI engines tend to operate at lean burn condition (φ < 1) for good fuel economy, but TWC suffers from low NOx conversion due to net oxidation condition (high O_2 concentration).

Exhaust gas recirculation (EGR) is a NOx control technique that controls combustion phasing and reduces combustion temperature through dilution effect, thermal effect, chemical effect, and mass-added effect. Dilution effect has a significant influence on NOx reduction via diluting O_2 in the intake charge, hence the lower adiabatic flame temperature. EGR phases the combustion process toward retard combustion (similar to retarded ignition timing) which increases cycle-to-cycle variation (reflects on coefficient of variation: COV of IMEP) and reduces combustion efficiency[16]. 20% EGR dilution rate can yield approximately 7% COV of IMEP and increases PM, THC and BSFC due mainly to the slower flame propagation velocity or laminar flame velocity (LFV). This helps to mitigate the knocking by reducing the rate of pressure change in the cylinder. The main challenges of the EGR system are the difficulty of controlling EGR flow rate[16–18] and the premature engine wear due to accelerated degrading lubrication oil problem[19–21].

Water injection is one of the combustion phasing control techniques that had been used in airplanes during the World War[22]. This technique can enhance output power and avoid knocking at wide open throttle (WOT) condition[22,23] using water's properties such as high heat of vaporisation, high heat capacity, and being inert in the combustion process. All properties mentioned enable intake charge cooling, reduce O_2 concentrations, increase heat capacity of intake charge which helps reduce rate of pressure change, peak pressure, peak temperature. Hence, knocking and NOx can be simultaneously suppressed[23,24]. Water injection also enables the engine control unit (ECU) to optimise the IGT to KLSA (Knock Limited Spark Advance) to obtain maximum brake torque (MBT), thus the engine can operate at higher IMEP[22,24].

There are three methods to introduce water into the combustion chamber: water/fuel emulsification, water port-injection (WPI), and direct water injection (DWI)[23,24]. Water/fuel emulsification uses emulsifier to create water/fuel solutions which existing fuel injection system can be used. However, the addition cost of emulsifier, phase instability of water/fuel, fixed water/fuel ratio are the main disadvantages. WPI and DWI have an advantage in terms of ability to adjust water/fuel ratio on-demand. WPI can be categorised into 1) single-point injection and 2) multi-point injection. Single-point WPI is simple to established and operate but creates an unequal water distribution among cylinders. Meanwhile, multi-point WPI can mitigate this problem and places water injectors closer to intake valves helping reduce water loss to wall impingement and yield near efficacy to DWI system[23,24]. DWI system can achieve high injection control flexibility and water metering accuracy, but high capital cost, high complexity, high energy cost, and cylinder liner impingement problem[24] seems to reduce its attractiveness.

With the literature reviews above, most research works focus on WPI system in turbocharged, high boost GDI engines operated with gasoline at high engine load[25,26]. Although, limited number of works pay attention to water injection on a natural-aspirated GDI engines fuelled with alternative fuel operated at medium to high load region. In this paper, the investigation on the effect of combustion phasing using a multi-point WPI system is carried out via an experimental approach. Combustion parameters and engine-out gaseous emissions are examined at MBT ignition timing baseline.

2. Experiment apparatus and research methodology

2.1. Engine test rig

The experimental setup is illustrated in **Figure 1** which employs a 4-cylinders GDI engine (Mazda Skyactiv G P3) mounted to a Lammed DW160H eddy-current dynamometer controlled by an FDJ-001 engine test rig controller for simulating engine load at constant speed and torque. The GDI engine's details are as shown in **Table 1**.

Table 1. GDI engine details.

Parameter	Details
Brand/Model	Mazda/Skyactiv G P3
Engine type	4 strokes, liquid cooled
No. of cylinder	4
Bore × stroke (mm)	71.0 × 82
Displacement (cm^3)	1298
Compression ratio	12.0:1
Continuous rated output	69.35 kW/5800 rpm
Maximum torque	123 Nm at 4000 rpm
Fuel injection	Direct injection

A Kistler: 6052C-3-1 (Switzerland) pressure sensor and a Kistler 2614CK (Switzerland) crank angle encoder is installed to the engine to measure in-cylinder pressure in respect to crank angular rotation. The signals from both sensors are processed by a combustion analyser of DEWESoft SIRIUSi-HS-CHG+ (Slovenia).

The GDI engine ignition and injection parameters are controlled by a Link G4 plus Force GDI engine ECU. The GDI injector used in the present study are multi-hole injectors with six nozzle holes. The injection timing and fuel pressure are set at 330° bTDC and 100 bar, respectively. Commercial grade Gasohol E20 (20% ethanol blended with gasoline) is used as fuel for this study. The characteristic of E20 is illustrated in **Table 2**.

Multi-hole fuel injectors are used in the present study for water injection which are controlled by a Tech 4 ECU-SHOP. The designated injection timing of 330° bTDC and the injection pressure of 3 bar are chosen. The water injectors are installed on the intake manifold where the distance from the water injector to the lower wall of the intake manifold is 35 mm with an impinging angle of 45°. This results in the horizontal distance from the water injector to the intake valve of approximately 130 mm.

Table 2. E20 fuel properties[27].

LHV (MJ/kg)	39.3
Density (kg/L)	0.757
RON	95.2
MON	83.4
C (%mass)	78
H (%mass)	13
O (%mass)	8
H/C ratio (molar)	2.000
O/C ratio (molar)	0.077

2.2. Emission measurement instruments

GDI engine-out gaseous emissions (HC, CO, NO_x, CO_2, and O_2) are quantified by a Horiba MEXA584L[28]. NO_x is measured by electrochemical methods. CO, HC, and CO_2 are measured by non-dispersed infrared absorption (NDIR) method. The measurement is taken 3 times with 1 minute interval after the engine has reached steady state to obtain an average reading of emissions.

For EGR dilution rate estimation, CO_2 concentrations at the intake manifold and exhaust manifold are measured and calculated using Equation (1)[29].

$$\%EGR = \frac{CO_{2,intake}}{CO_{2,exhaust}} \times 100\% \quad (1)$$

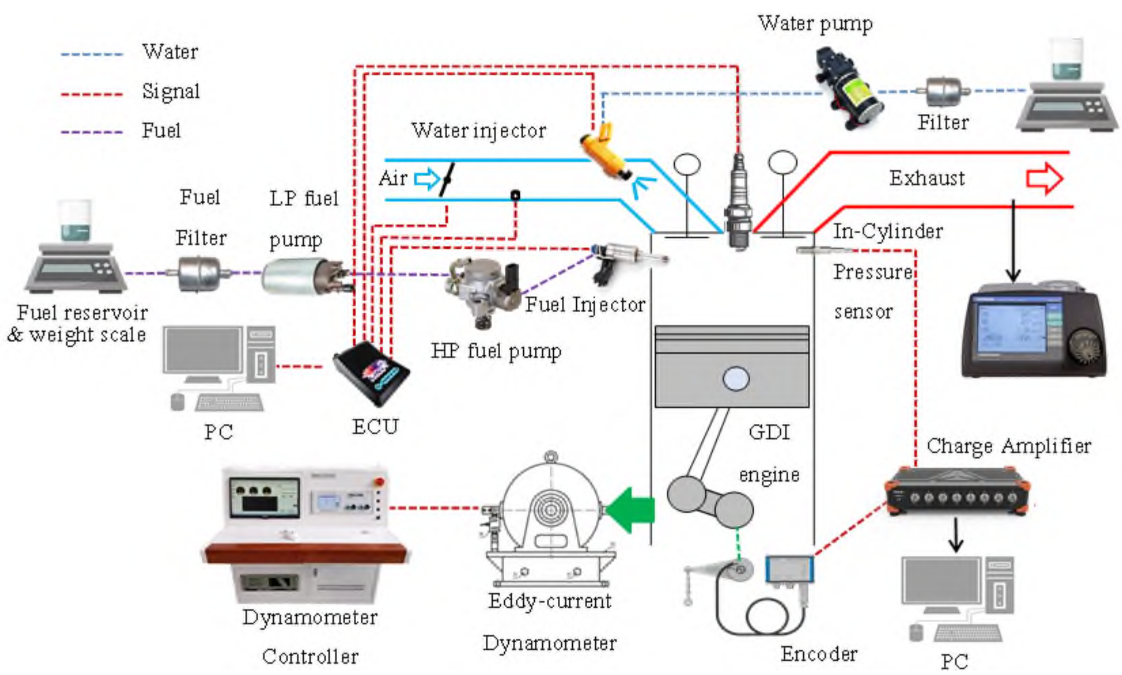

Figure 1. Schematic of the experimental setup.

2.3. Experiment procedures and conditions

a) The engine is operated at a constant speed of 2000 rpm (±5%) and with the indicated mean effective pressure (IMEP) of 6 bar corresponding to engine load of approximately 75%.

b) Firstly, the sweep test is performed to mainly observe the effect of ignition timing (IGT) on engine brake torque which determines the maximum brake torque (MBT)[30] ignition timing. This condition is then assumed to be the 'baseline' condition.

c) Then, water injection (abbreviated: H_2O_inj) is commenced with the MBT IGT (in this case, IGT MBT = 12CA bTDC) from 1.0 ms to 5.5 ms which is corresponding to approximately 5% to 30% of fuel (E20) mass injected at baseline condition. This is done to evaluate the effect of water injection on NOx reduction (deNOx), other gaseous emissions, and combustion parameters.

d) After the H_2O injection sweep tests, the GDI engine is allowed to return to the baseline condition again for 10 minutes before adding EGR. The EGR dilution rate of approximately 10% is performed as a benchmark for the deNOx performance. Then, IGT is adjusted to have Peak Pressure Position (PPP) matches with that of baseline condition. The comparison between engines operated with EGR and H_2O injection is evaluated based on the assumptions of equivalence deNOx and optimised IGT. Optimised IGT is based on the timing that MBT is achieved[30].

e) The GDI engine is operated in homogeneous combustion mode and is controlled fuel injection rate to achieve stoichiometric equivalence ratio (φ = 1, ±0.005).

2.4. Data processing and analysis

The net rate of heat release (RoHR or HRR) is computed using an average in-cylinder pressure value of 300 cycles. HRR is calculated using MS Excel spreadsheet via Equation (2)[15].

$$\frac{dQ}{d\theta} = \frac{\gamma}{\gamma - 1} p \frac{dV}{d\theta} + \frac{1}{\gamma - 1} V \frac{dP}{d\theta} \quad (2)$$

Where, $dQ/d\theta$ = net rate of heat release (J/θ), γ = coefficient of isentropic expansion, P = current in-cylinder pressure (Pa), $dV/d\theta$ = rate of in-cylinder volume change (m^3/θ), V = current in-cylinder volume (m^3), and $dP/d\theta$ = rate of in-cylinder pressure change (Pa/θ).

Mass fraction burned (MFB) of fuel in the combustion process is calculated using HRR spreadsheet which enables the observation of ignition delay, position where 50% of fuel mass is burned (MFB50), and combustion duration (CA1090).

Meanwhile, Indicated Mean Effective Pressure (IMEP), Coefficient of Variance of IMEP (COV of IMEP), maximum in-cylinder pressure (Pmax), and location of Pmax are computed using an in-house developed MATLAB script.

3. Results and discussions

3.1. Effect of IGT

Figure 2 illustrates the effect of IGT change on in-cylinder pressure profile and HRR. The increase in IGT demonstrates the rise of in-cylinder pressure and the left-shift toward an advanced combustion process. The advanced ignition timing results in rapid pressure development, hence the higher peak pressure. Note that subtle knocking noise is audible without special equipment at IGT of 13 CA bTDC and the obvious knocking noise can be heard at IGT of 15 CA bTDC. The rate of pressure change ($dP/d\theta$) depicts the substantial $dP/d\theta$ prior TDC for IGT = 15 that suggests the potential knocking event. Although, this is considered a mild knocking compared to previous authors[31,32] who experimented on significantly higher engine load (IMEP > 15 bar). Additionally, the use of smoothed pressure trace has averaged-out the anomaly pressure rise from the in-cylinder pressure profile data acquired. Therefore, the $dP/d\theta$ curves in **Figure 2** are visually smooth and knocking even is undetected.

Increasing IGT results in combustion phasing toward advanced combustion which moves the centre of combustion (MFB50 or CA50) closer to TDC as shown in **Figure 3**. IGT and position of MFB50 demonstrate overall linear relationship which MBT IGT based on MFB50 = 10 CA aTDC[30] can be calculated from empirical linear Equation (3) derived from the experiment.

$$MFB50 = (-1.2531 \cdot IGT) + 21.683 \qquad R^2 = 0.9907 \tag{3}$$

The calculated IGT optimised for MBT is 9.32 CA bTDC, however, according to the brake torque profile in **Figure 4**, the brake torque is far from peak value. Therefore, the IGT value of 12 CA bTDC is chosen based on Heywood's assumption of MBT[6]. This results in MFB50 of approximately 7 CA aTDC which is considered in an optimal range for SI engine)[24].

The peak in-cylinder pressure (Pmax) is depicted in **Figure 4** which increases with the advanced IGT value. Advancing IGT leads to early combustion of the intake mixture and produces high temperature and pressure hot gas closer to TDC, resulting in higher Pmax value. Note that higher Pmax and the shift Pmax toward TDC increases negative work of the engine and can reduce net positive work, hence the lower output brake torque.

BTE reaches the peak value at MBT IGT (IGT = 12) as the result of optimal combustion while advancing or retarding ignition timing from this value indicates a noticeable BTE decrease. Overall, the combustion is sufficiently stable with COV of IMEP below 5% except for the condition of IGT = 6 which late combustion negatively affects the combustion stability. Meanwhile, the combustion efficiency demonstrates a slight drop over the increasing IGT.

Advancing IGT results in a significant increase in NOx concentration which 46% NOx increase over IGT sweep of 9 CA as depicted in **Figure 5**. The increase of IGT results in a substantial rise of peak in-cylinder pressure (Pmax) (as shown in **Figure 4**) which effectively increases the in-cylinder peak temperature. Hence, the formation of thermal NOx is enhanced and yields higher engine-out NOx concentration.

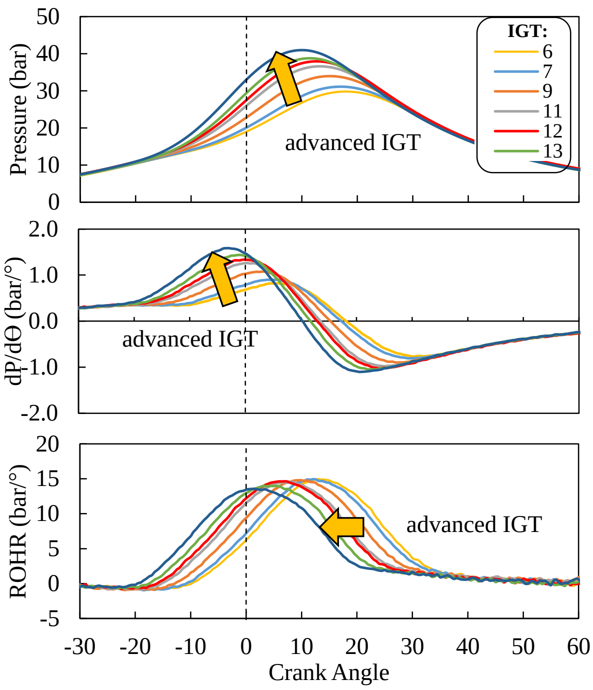

Figure 2. Effect of IGT on P_{cyl}, $dP/d\theta$ & HRR.

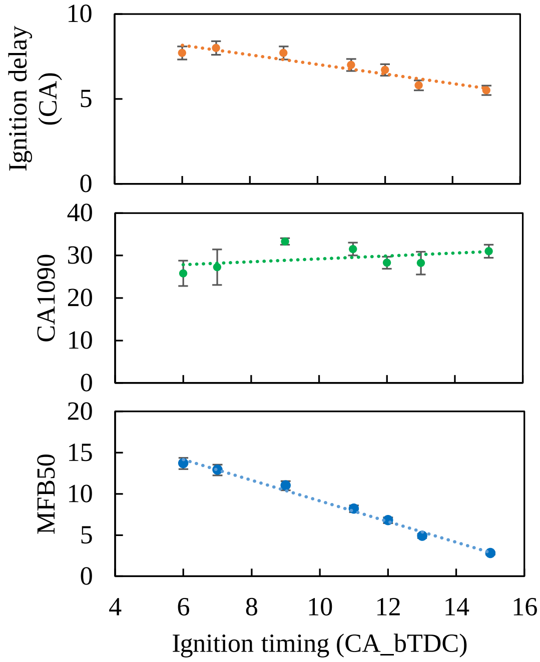

Figure 3. Effect of IGT on combustion parameters.

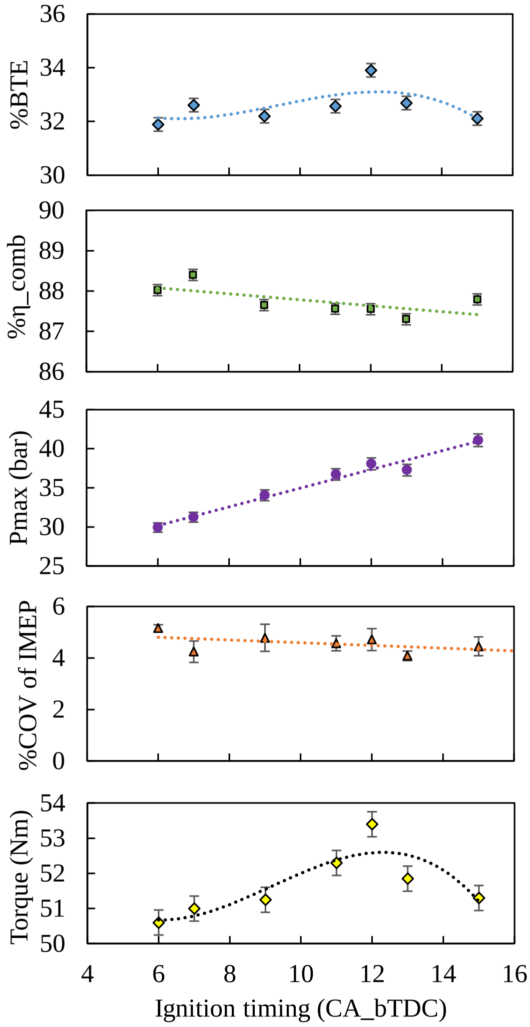

Figure 4. Effect of IGT on GDI engine parameters.

THC concentration indicates a considerable increase with the advanced combustion as a result of high peak in-cylinder pressure that encourages hydrocarbon specie to get trap into the crevice volume[24] during expansion stroke and then gets expelled into exhaust gas stream during exhaust stroke.

CO concentration exhibits a similar trend to that of THC concentration which reflects the combustion process incompleteness. Combustion efficiency (η_c or η_{comb}) is defined in (4).

$$\eta_c = \frac{CO_2}{CO + CO_2} \times 100\% \tag{4}$$

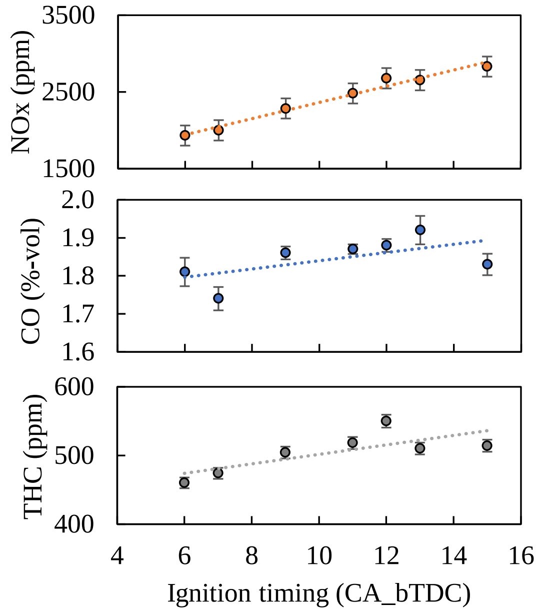

Figure 5. Effect of IGT on engine-out emissions.

3.2. Effect of H_2O injection

After the MTB IGT is established from the previous section (12 CA bTDC), the experiment with water injection is performed from 1.0 ms to 5.5 ms (corresponding to 5% to 30% mass fuel injected) without IGT adjustment to observe the effect of water injection on engine performances. The increased amount of water injected results in the lowered magnitude and the retarded of in-cylinder pressure which consequently decrease the peak of heat release rate and late combustion process as illustrated in **Figure 6**. The introduction of water significantly reduces the rate of pressure change which indicates the potential of suppression knocking.

Water addition into the combustion chamber results in the longer ignition delay, prolonged combustion duration and MFB50 shifted to later in the combustion process as shown in **Figure 7**. This is due mainly to the property of water (e.g. high heat capacity, high heat of vaporisation, and being inert fraction in the combustion chamber) that decreases the temperature of the combustion via heat absorption and chemical effect, hence the observable decrease of in-cylinder pressure[24].

It can be seen at the condition with the water injection of 5.5 MS, MFB50 is shifted to 15 CA aTDC which is considered as significant late combusting and required advancing IGT to correct MFB50 back to 7 CA aTDC for MBT condition[30]. The presence of water vapour in the combustion chamber decreases the laminar flame velocity during the early combustion process[33]. However, combustion duration (CA1090) indicates an insignificant increase trend compared to that of ignition delay and MFB50 which significantly increase with the high rate of water injection.

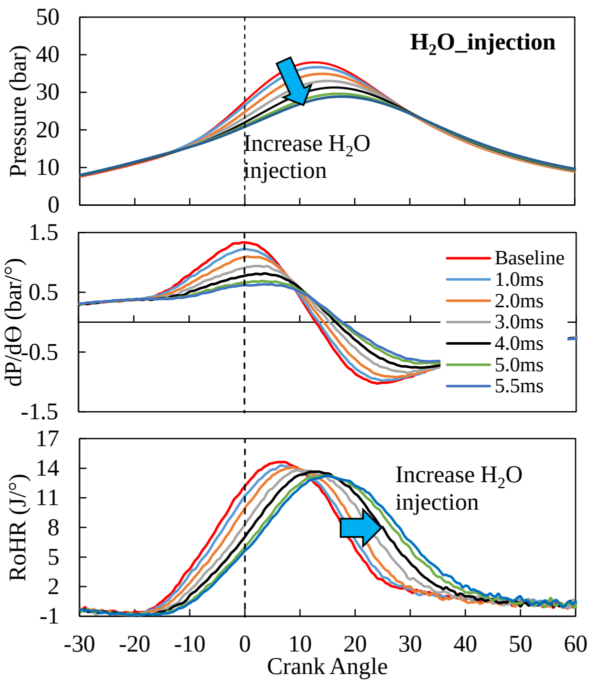

Figure 6. Effect of H_2O injection on combustion characteristics.

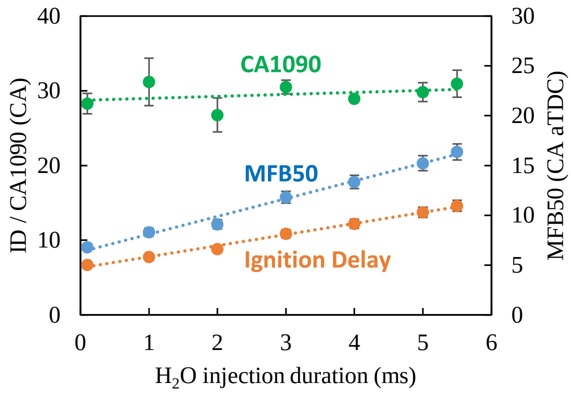

Figure 7. Effect of H_2O injection on combustion parameters.

The introduction of water results in the noticeable reduction in combustion efficiency and BTE (as shown in **Figure 8**) as a result of deteriorated combustion process[23,34]. However, the COV of IMEP specifies lower than 5% which suggests that more water could be injected before the limit of combustion stability has reached. The effect of water injection quantity on deNOx performance which can be observed as a linear function from 1 ms and up to approximately 4 ms of injector turn-on duration. This is corresponding to 25% to 82% of NOx reduction achievable. The reduction in NOx concentration is due mainly to the reduced in-cylinder peak temperature[25] caused by the combination of charge dilution effect[24] and additional charge cooling effect[23,32]. The reduced peak of HRR also contributes to the reduction of NOx emission. Additionally, the generation of hydrogen radical (H) and oxygen radical (e.g. O and OH) is suppressed by H_2O injection due to chemical equilibrium[35]. However, the further water injection quantity from this point (from 5 ms onward or 25% H_2O, approx.) is deemed as a 'diminishing return' in which the effort to reduce NOx increases significantly, but the deNOx only moderately improves. The higher cost to reduce NOx is supported by the steady increase of CO and THC concentrations as a larger mass of water is injected as illustrated in **Figure 8**.

CO concentration visibly rises when H_2O injection rate increases from 1 ms to 2 ms as the result of deteriorated combustion process. Another reason for the higher CO concentration is the dilution effect caused by water vapour that replaces O_2 and yields a lowered O_2 concentration in the intake charge[32]. Hence, CO is prevented from complete oxidation into CO_2.

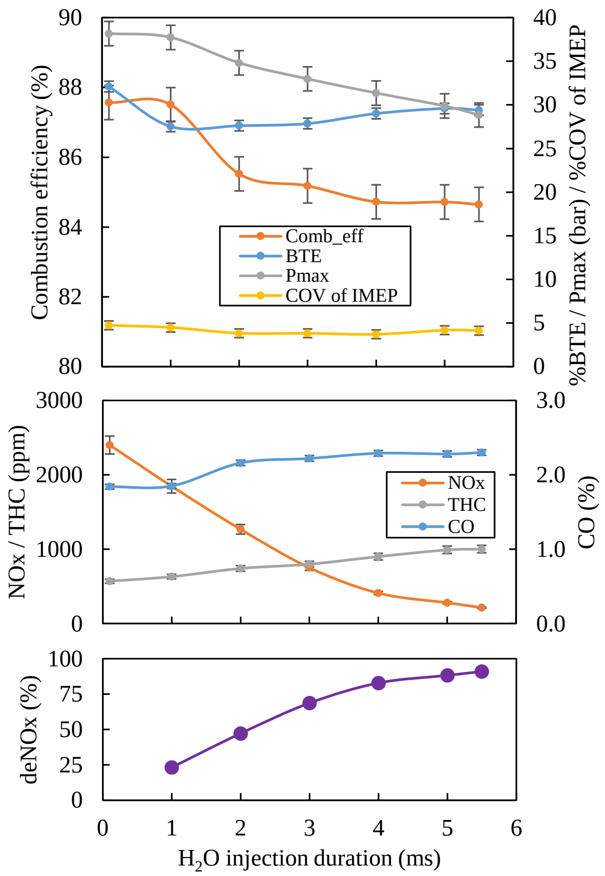

Figure 8. Effect of H_2O injection on GDI engine performances.

THC concentration moderately increases with the large quantity of water injected due to several reasons. Firstly, the lowered in-cylinder temperature caused by the charge cooling effect of water encourages flame quenching which increases unburned THC[22,25,35]. Water droplets that are unable to fully vaporise could impinge onto the cylinder liner and absorb heat which reduces cylinder wall temperature, hence the increased flame quench. Secondly, the lowered in-cylinder temperature combined with the O_2-poor diluted intake charge reduces the post-combustion oxidation of unburned THC. Thirdly, water injection reduces flame laminar velocity as evidence of the longer ignition delay in **Figure 7**. This means that flame kernel development could be negatively affected and leads to the cycle-to-cycle variation[35]. Misfire could occur as the result of prolonged ignition delay. Although, the COV of IMEP suggests that the intensity of cycle-to-cycle variation is still below the 5% threshold. Therefore, THC generated from cycle-to-cycle variation is insignificant compared to that of flame quenching.

As CO and THC are relatively simpler to control than NOx because they can be oxidised effectively at lean AFR[36]. On the other hand, aftertreatment deNOx (e.g. TWC) requires ‘net reduction’ condition[37] (rich AFR = poor O_2) to reduce NOx into harmless N_2. NOx reduction technique that utilises period rich-lean AFR cycle usually results in fuel penalty. Therefore, the increase in CO and THC concentrations become secondary concerns when compared to worsening BTE (and BSFC) and combustion stability.

3.3. Combined effect of IGT and H_2O injection

In the previous section, 30% rate of water injection is experimented at IGT = 12 with acceptable combustion stability and other combustion parameters considered. Afterwards, the effect of IGT on GDI engines with H_2O injection is investigated. IGT is increased until the same location of peak pressure (LPP) as MBT condition is met (approx. 12 CA aTDC). In this case, the IGT is swept from 12 CA aTDC to 19 CA aTDC which results in LPP of 12 CA aTDC ±0.2CA as shown in the traces of in-cylinder pressure in **Figure 9**. The *dP/dθ* curves reveal that water injection is capable of suppressing knock by reducing the maximum rate of pressure rise by 35% from baseline condition. For comparison, at baseline condition in section 3.1, subtle audible knocking noise could be observed from the IGT = 13. Meanwhile, with 30% H_2O injection, IGT can be adjusted to 19 CA bTDC without knocking.

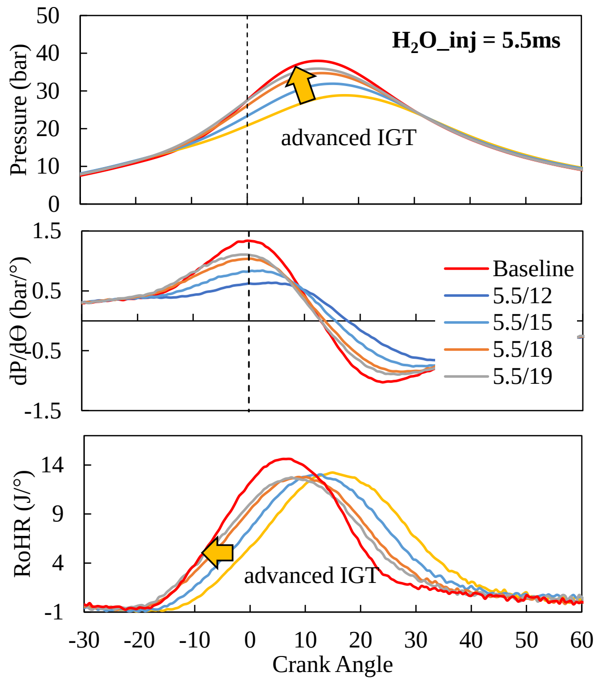

Figure 9. Effect of IGT and H_2O injection on combustion characteristics.

Overall, the effect of IGT on the combustion process presented in this section closely resembles the results in section 3.1. However, the main difference could be seen with the sensitivity of the effect of IGT on ignition delay. In absence of H_2O, the advance in IGT by 3.8 CA yields 1 CA of ignition delay shortened as illustrated in **Figure 10**. Meanwhile, in the presence of H_2O, it would take almost twice as much IGT advance to yield the same reduction of ignition delay duration. It can be concluded that the presence of H_2O exhibits a noticeable negative effect on early flame development due to the charge dilution effect. Compounded with heat absorption by water's vaporisation process (charge cooling effect), this results in the longer duration of flame kernel to initiate and stabilise[25]. The same trend of the sensitivity of IGT advance on MFB50 is observed as the effect of IGT on MFB50 is more pronounced for baseline conditions than that of conditions with H_2O injection.

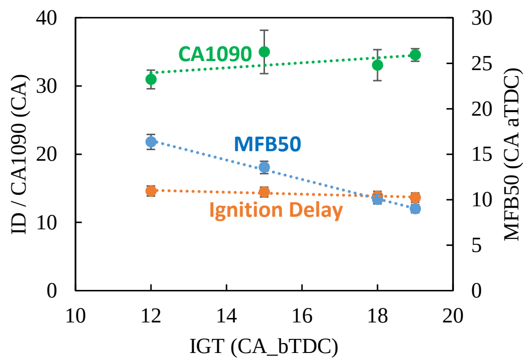

Figure 10. Effect of IGT and H_2O injection on combustion parameters.

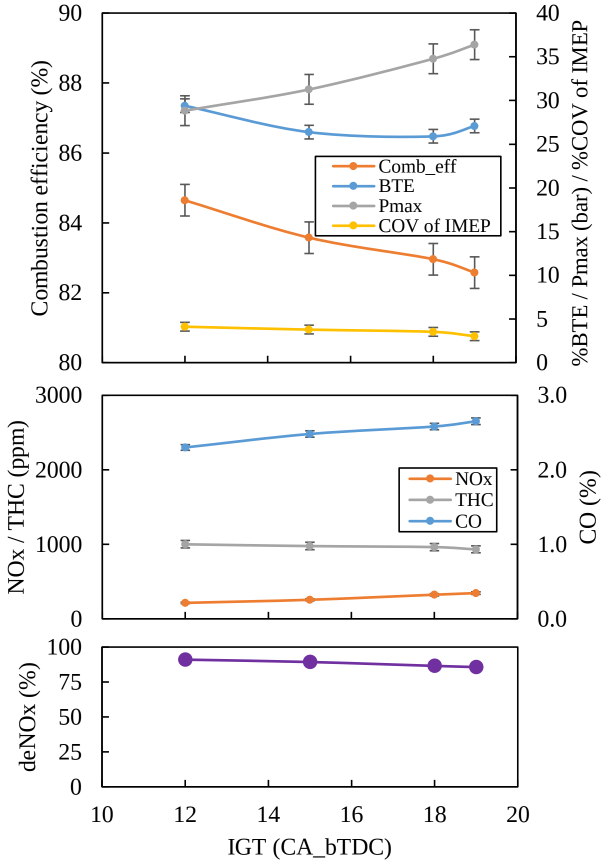

Figure 11. Effect of IGT and H_2O injection on GDI engine performances.

While ignition delay and MFB50 values decrease with advanced IGT, combustion duration indicates a slight increase. The slight rising trend of CA1090 by IGT reported in this investigation demonstrates an opposite trend to most previous research works reviewed[22,24,25,31,32,34,35,38–40]. Still, there are researchers who reported that longer CA1090 caused by advancing IGT[41,42]. It is speculated that the dilution effect and cooling effect of water injection at specified condition (30% H_2O injection) affects combustion phasing and can no longer be compensated by solely advancing IGT.

In general, advancing IGT leads to the higher Pmax as described in section 3.1 which increases the in-cylinder temperature. Consequently, NOx concentration marginally rises as the result of enhanced generation of thermal NOx. From the perspective of deNOx, advancing IGT slightly demerits the benefit of injecting water on deNOx. However, improvements on cycle-to-cycle variation, and THC emission could be observed in **Figure 11**. Therefore, advancing IGT can be performed at a relatively low penalty of deNOx performance.

The increase in CO concentration with more advanced combustion indicates poorer combustion efficiency which strongly correlates to insufficient O_2 environment in the combustion chamber. 30% H_2O injection results in a noticeably increase in equivalence ratio (ϕ) up to 1.04 indicating a richer AFR which is caused by the charge dilution effect of water vapour that reduced O_2 concentration in the intake charge. Another plausible reason for the elevated CO concentration is due to the early combustion leading to lower exhaust gas temperature compared to that of late combustion. Consequently, the post-combustion oxidation of CO into CO_2 is less pronounced.

3.4. Comparison between EGR and H_2O injection

As deNOx performance baseline by H_2O injection has been established in section 3.1 and 3.2, it is crucial to obtain a better understanding of its merits in comparison to proven NOx control techniques: EGR.

10% EGR dilution rate is chosen as a benchmark against H_2O injection technique in this investigation. The comparison between the two deNOx methods is performed based on the same value of deNOx for a fair comparison. Empirical equations of NOx emission characteristic obtained from H_2O injection experiment (**Figure 8**) is as shown in Equation (5).

$$NOx = -2.6842x^4 + 36.887x^3 - 99.6x^2 - 526.04x + 2450.1$$
$$R^2 = 0.9997 \tag{5}$$
Note: x = H_2O injection duration in ms

At 10% EGR rate and IGT = 12, the deNOx is 82%. NOx concentration at baseline condition is 2400 ppm, hence the 82% NOx reduction yields 1968 ppm NO reduced (432 ppm NOx remains). Using Equation (5), the author obtains the H_2O injection duration of 3.94 ms. Therefore, the results from H_2O injection experiment condition of 4 ms (corresponding to 20% W/F) is chosen to compare with the results of 10%EGR. Details of parameters for the comparison are shown in **Table 3**.

Table 3. Comparison conditions between EGR and H_2O injection.

Parameter	**EGR**	**H_2O injection**
Dilution rate/injection rate	10%	20% W/F (4.0 ms)
IGT baseline	12 CA bTDC	12 CA bTDC
IGT optimised*	15 CA bTDC	18 CA bTDC

*IGT is adjusted to obtain same LPP as baseline condition (LPP = 12 CA aTDC, approx.).

Figure 12 illustrates the comparison of in-cylinder pressure traces, *dP/dθ* curves, and HRR curves between GDI engine baseline, 10%EGR, and 20% H_2O injection. Without the IGT optimisation, both peak pressure and *dP/dθ* of EGR and H_2O injection are remarkably lower than that of baseline condition. In-cylinder pressure trace of H_2O injection also indicates a further peak pressure reduction compared to that of EGR. This suggests that at the same %deNOx, H_2O injection would be more potent in suppression knocking compared to EGR.

With optimised IGT, the new pressure traces for either EGR and H_2O injection are nearly identical to baseline condition in terms of pressure magnitude and location. However, the peak *dP/dθ* curves for EGR and H_2O injection are marginally lower than baseline which specifies the lower rate of temperature rise in the combustion chamber. The HRR curves between baseline conditions, EGR @ IGT = 15, and H_2O injection @ IGT = 18, further confirms that heat is released at a substantially lower rate which results in thermal NOx inhibition as shown in the relative emissions in **Figure 13**.

Without IGT optimisation (IGT = 12) (denoted ‘MBT’), 10%EGR yields NOx reduction of 82% while optimised IGT (denoted ‘opt’) shows NOx reduction of 77% due to higher *dP/dθ* and Pmax (**Figure 13**) that generates more NOx.

DeNOx strategy using H_2O injection demonstrates significantly better CO emission compared to EGR. This means EGR has more aggressive dilution which in turn replaces more O_2 molecules and causes O_2 deprivation combustion process. On the other hand, H_2O injection utilises both dilution effect and charge cooling effect to achieve the same NOx reduction. Meanwhile, H_2O injection generates considerably higher THCs than that of EGR as the results of poorer early flame kernel development as indicated by the longer ignition delay in **Figure 13**. MBF50 and CA1090 are comparable for both H_2O injection and EGR when IGT is optimised.

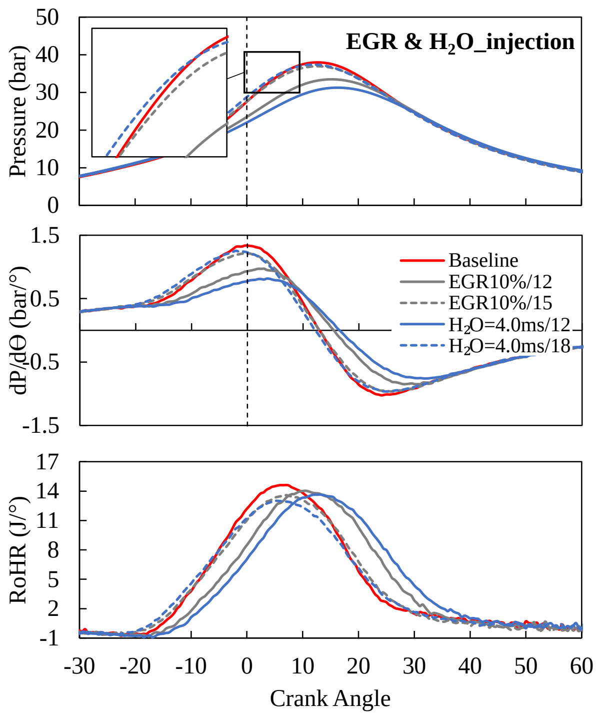

Figure 12. Combustion parameters comparison between EGR and H_2O injection.

Overall, H_2O injection technique demonstrates a promising performance as NOx reduction techniques compared to advanced and matured technique like EGR.

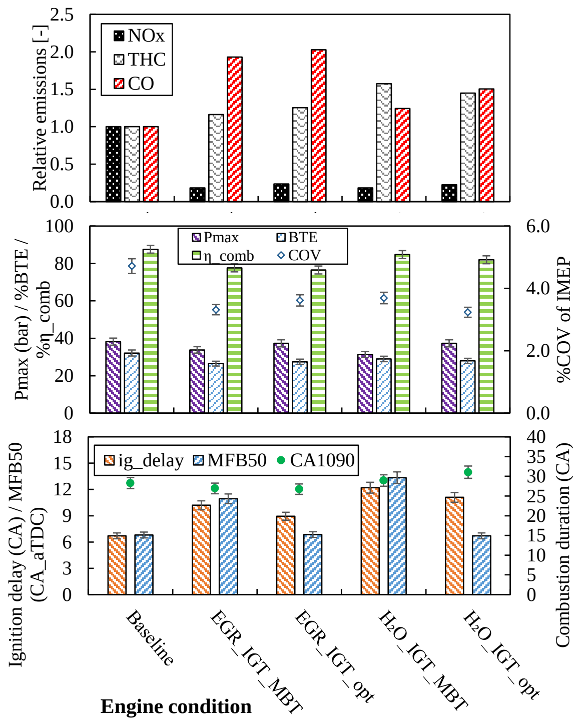

Figure 13. Comparison between EGR and H_2O injection

4. Conclusions

The higher engine load and lowered RPM operation of the modern 'down-sized' gasoline direct injection engine has led to high amounts of NOx and knocking problems. The investigation on the effect of water injection on GDI engine performances at high load is carried out via an experimental approach to solve

NOx and knocking problem. The results indicate that water injection is capable of simultaneously suppressing NOx and knocking while maintaining reasonable brake thermal efficiency and combustion stability in comparison to that of EGR technology. Water injection technique has potential to be employed in boarder commercial road vehicles as a clean ICE technology during the transition into electrification transports. Future work will be devoted to a deeper understanding of the effect of water injection on particulate matter emissions and the aftertreatment system.

5. Acknowledgments

This research was funded by National Science, Research and Innovation Fund (NSRF), and King Mongkut's University of Technology North Bangkok with Contract no. KMUTNB-FF-66-19.

Conflict of interest

The authors declare no conflict of interest.

References

1. Lindsey R, Dahlman LA. Climate change: Global temperature. Available online: https://www.climate.gov/news-features/understanding-climate/climate-change-global-temperature (accessed on 31 July 2023).
2. Xie R, Fang J, Liu C. The effects of transportation infrastructure on urban carbon emissions. *Applied Energy* 2017; 196: 199–207. doi: 10.1016/j.apenergy.2017.01.020
3. Kittelson DB. Engines and nanoparticles: A review. *Journal of Aerosol Science* 1998; 29(5–6): 575–588. doi: 10.1016/S0021-8502(97)10037-4
4. Amelang S, Wehrmann B. "Dieselgate"—A timeline of the car emissions fraud scandal in Germany. *Clean Energy Wire* 2020.
5. Pulkrabek WW. *Engineering Fundamentals of the Internal Combustion Engine*, 2th ed. New Jersey: Pearson Prentice-Hall; 2004.
6. Heywood JB. *Internal Combustion Engine Fundamentals*. New York: McGraw-Hill; 1988.
7. Jiang C, Xu H, Srivastava D, et al. Effect of fuel injector deposit on spray characteristics, gaseous emissions and particulate matter in a gasoline direct injection engine. *Applied Energy* 2017; 203: 390–402. doi: 10.1016/j.apenergy.2017.06.020
8. Hergueta C, Bogarra M, Tsolakis A, et al. Butanol-gasoline blend and exhaust gas recirculation, impact on GDI engine emissions. *Fuel* 2017; 208: 662–672. doi: 10.1016/j.fuel.2017.07.022
9. Wang C, Xu H, Herreros JM, et al. Fuel effect on particulate matter composition and soot oxidation in a Direct-Injection Spark Ignition (DISI) engine. *Energy & Fuels* 2014; 28(3): 2003–2012. doi: 10.1021/ef402234z
10. Williams M, Minjares R. *A technical summary of Euro 6/VI vehicle emission standards*. International Council on Clean Transportation (ICCT); 2016.
11. Mock P. *CO_2 Emission Standards for Passenger Cars and Light-Commercial Vehicles in the European Union*. International Council on Clean Transportation (ICCT); 2019.
12. Shi Y, Cai Y, Fan R, et al. Characterization of soot inside a diesel particulate filter during a nonthermal plasma promoted regeneration step. *Applied Thermal Engineering* 2019; 150: 612–619. doi: 10.1016/j.applthermaleng.2019.01.015
13. Wang Y, Wei H, Zhou L, et al. *Effect of Injection Strategy on the Combustion and Knock in a Downsized Gasoline Engine with Large Eddy Simulation*. SAE Technical Paper; 2020.
14. Xia F, Griefnow P, Tidau F, et al. Electric torque assist and supercharging of a downsized gasoline engine in a 48V mild hybrid powertrain. *Proceedings of the Institution of Mechanical Engineers, Part D: Journal of Automobile Engineering* 2020; 235(5): 1245–1255. doi: 10.1177/0954407020968956
15. Stone R. *Introduction to Internal Combustion Engines*, 4th ed. Springer; 2012.
16. Wei H, Zhu T, Shu G, et al. Gasoline engine exhaust gas recirculation—A review. *Applied Energy* 2012; 99: 534–544. doi: 10.1016/j.apenergy.2012.05.011
17. Liu F, Pfeiffer J. Estimation algorithms for low pressure cooled EGR in spark-ignition engines. *SAE International Journal of Engines* 2015; 8(4): 1652–1659.
18. Asano I. Measurement Systems for Diesel Exhaust Gas and Future Trends. Available online: http://www-origin.horiba.com/uploads/media/RE03-03-012-600.pdf (accessed on 31 July 2023).
19. Pandey AK, Nandgaonkar M, Suresh S. *Comparison and Evaluation of Engine Wear, Performance, NOx Reduction and Nano Particle Emission of Diesel, Karanja and Jatropha Oil Methyl Ester Biodiesel in a Military720 kW, heavy duty CIDI Engine Applying EGR with Turbo Charging*. SAE Technical Paper; 2020.
20. Singh SK, Agarwal AK, Sharma M. Experimental investigations of heavy metal addition in lubricating oil and

soot deposition in an EGR operated engine. *Applied Thermal Engineering* 2006; 26(2–3): 259–266. doi: 10.1016/j.applthermaleng.2005.05.004
21. Aldajah S, Ajayi OO, Fenske GR, Goldblatt IL. Effect of exhaust gas recirculation (EGR) contamination of diesel engine oil on wear. *Wear* 2007; 263(1–6): 93–98. doi: 10.1016/j.wear.2006.12.055
22. Zhuang Y, Sun Y, Huang Y, et al. Investigation of water injection benefits on downsized boosted direct injection spark ignition engine. *Fuel* 2020; 264: 116765. doi: 10.1016/j.fuel.2019.116765
23. Zhu S, Hu B, Akehurst S, et al. A review of water injection applied on the internal combustion engine. *Energy Conversion and Management* 2019; 184: 139–158. doi: 10.1016/j.enconman.2019.01.042
24. Wan J, Zhuang Y, Huang Y, et al. A review of water injection application on spark-ignition engines. *Fuel Processing Technology* 2021; 221: 106956. doi: 10.1016/j.fuproc.2021.106956
25. Golzari R, Zhao H, Hall J, et al. Impact of intake port injection of water on boosted downsized gasoline direct injection engine combustion, efficiency and emissions. *International Journal of Engine Research* 2019; 22(1): 295–315. doi: 10.1177/1468087419832791
26. Wang C, Zhang F, Wang E, et al. Experimental study on knock suppression of spark-ignition engine fuelled with kerosene via water injection. *Applied Energy* 2019; 242: 248–259. doi: 10.1016/j.apenergy.2019.03.123
27. De Simio L, Gambino M, Iannaccone S. Effect of ethanol content on thermal efficiency of a spark-ignition light-duty engine. *ISRN Renewable Energy* 2012; 2012. doi: 10.5402/2012/219703
28. Duan X, Zhang S, Liu Y, et al. Numerical investigation the effects of the twin-spark plugs coupled with EGR on the combustion process and emissions characteristics in a lean burn natural gas SI engine. *Energy* 2020; 206: 118181. doi: 10.1016/j.energy.2020.118181
29. Zhang J, Yu X, Guo Z, et al. Effect of exhaust gas recirculation and spark timing on combustion and emission performance of an oxygen-enriched gasoline engine. *ACS Omega* 2022; 7(46): 42208–42220. doi: 10.1021/acsomega.2c05034
30. Eriksson L. *Spark Advance Modeling and Control* [PhD thesis]. Linköping University; 1999.
31. Li A, Zheng Z, Peng T. Effect of water injection on the knock, combustion, and emissions of a direct injection gasoline engine. *Fuel* 2020; 268: 117376. doi: 10.1016/j.fuel.2020.117376
32. Kim J, Park H, Bae C, et al. Effects of water direct injection on the torque enhancement and fuel consumption reduction of a gasoline engine under high-load conditions. *International Journal of Engine Research* 2016; 17(7): 795–808. doi: 10.1177/1468087415613221
33. Cazzoli G, Falfari S, Bianchi GM, Forte C. Development of a chemical-kinetic database for the laminar flame speed under GDI and water injection engine conditions. *Energy Procedia* 2018; 148: 154–161. doi: 10.1016/j.egypro.2018.08.043
34. Mingrui W, Sa NT, Turkson RF, et al. Water injection for higher engine performance and lower emissions. *Journal of the Energy Institute* 2017; 90(2): 285–299. doi: 10.1016/j.joei.2015.12.003
35. Wang J, Duan X, Liu Y, et al. Numerical investigation of water injection quantity and water injection timing on the thermodynamics, combustion and emissions in a hydrogen enriched lean-burn natural gas SI engine. *International Journal of Hydrogen Energy* 2020; 45(35): 17935–17952. doi: 10.1016/j.ijhydene.2020.04.146
36. Easter J, Bohac SV. Three way catalyst-selective catalytic reduction aftertreatment system evaluation for a lean burn gasoline engine operating in homogenous charge compression ignition, spark-assisted compression ignition, and spark-ignited combustion modes. *Journal of Engineering for Gas Turbines and Power* 2018; 140(12). doi: 10.1115/1.4039424
37. Oh SH, Triplett T. Reaction pathways and mechanism for ammonia formation and removal over palladium-based three-way catalysts: Multiple roles of CO. *Catalysis Today* 2014; 231: 22–32. doi: 10.1016/j.cattod.2013.11.048
38. Anufriev IS. Review of water/steam addition in liquid-fuel combustion systems for NOx reduction: Waste-to-energy trends. *Renewable and Sustainable Energy Reviews* 2021; 138: 110665. doi: 10.1016/j.rser.2020.110665
39. Hoppe F, Thewes M, Seibel J, et al. Evaluation of the potential of water injection for gasoline engines. *SAE International Journal of Engines* 2017; 10(5): 2500–2512. doi: 10.4271/2017-24-0149
40. Xu P, Ji C, Wang S, et al. Effects of direct water injection on engine performance in engine fueled with hydrogen at varied excess air ratios and spark timing. *Fuel* 2020; 269: 117209. doi: 10.1016/j.fuel.2020.117209
41. d'Adamo A, Berni F, Breda S, et al. *A Numerical Investigation on the Potentials of Water Injection as a Fuel Efficiency Enhancer in Highly Downsized GDI Engines*. SAE Technical Paper; 2015.
42. Vacca A, Bargende M, Chiodi M, et al. *Analysis of Water Injection Strategies to Exploit the Thermodynamic Effects of Water in Gasoline Engines by Means of a 3D-CFD Virtual Test Bench*. SAE Technical Paper; 2015.